Departmental Papers (MSE)                  Department of Materials Science & Engineering

February 2006

# Construction, assessment, and application of a bond-order potential for iridium

Marc J. Cawkwell
*University of Pennsylvania*

Duc Nguyen-Manh
*Culham Science Centre*

David G. Pettifor
*University of Oxford*

Vaclav Vitek
*University of Pennsylvania*, vitek@lrsm.upenn.edu

Follow this and additional works at: https://repository.upenn.edu/mse_papers

## Recommended Citation

# Construction, assessment, and application of a bond-order potential for iridium

## Abstract

A tight-binding based bond-order potential (BOP) has been constructed for the fcc transition metal iridium that includes explicitly only *d* orbitals in the evaluation of the total energy. We show that hybridization between the nearly free electron *sp* band and the unsaturated covalently bonded *d* orbitals is important in determining the relative stabilities of the close-packed structures and that this effect can be accurately captured through the use of a central force term. The BOP is found to provide an excellent description of the equilibrium properties of iridium, including its negative Cauchy pressure that is fitted using a many-body repulsive term. The transferability of the BOP is assessed by calculating energy differences between different crystal structures, the energetics of the tetragonal and trigonal deformation paths, the phonon spectra, stacking fault, and vacancy formation energies. Comparison of the results of these studies with either experiments or first principles calculations is found to be good. We also describe briefly the application of the constructed BOP to the atomistic simulation of the core structure of the screw dislocation that led to an explanation of the anomalous deformation and fracture behavior exhibited of iridium.

## Comments

# Construction, assessment, and application of a bond-order potential for iridium

M. J. Cawkwell,[1,*] D. Nguyen-Manh,[2,†] D. G. Pettifor,[3] and V. Vitek[1,‡]

[1]*Department of Materials Science and Engineering, University of Pennsylvania, 3231 Walnut Street, Philadelphia, Pennsylvania 19104-6202, USA*

[2]*EURATOM/UKAEA Fusion Association, Culham Science Centre, Abingdon, OX14 3DB, United Kingdom*

[3]*Department of Materials, University of Oxford, Parks Road, Oxford, OX1 3PH, United Kingdom*

A tight-binding based bond-order potential (BOP) has been constructed for the fcc transition metal iridium that includes explicitly only $d$ orbitals in the evaluation of the total energy. We show that hybridization between the nearly free electron $sp$ band and the unsaturated covalently bonded $d$ orbitals is important in determining the relative stabilities of the close-packed structures and that this effect can be accurately captured through the use of a central force term. The BOP is found to provide an excellent description of the equilibrium properties of iridium, including its negative Cauchy pressure that is fitted using a many-body repulsive term. The transferability of the BOP is assessed by calculating energy differences between different crystal structures, the energetics of the tetragonal and trigonal deformation paths, the phonon spectra, stacking fault, and vacancy formation energies. Comparison of the results of these studies with either experiments or first principles calculations is found to be good. We also describe briefly the application of the constructed BOP to the atomistic simulation of the core structure of the screw dislocation that led to an explanation of the anomalous deformation and fracture behavior exhibited of iridium.

PACS number(s): 61.50.Ah, 61.72.Bb, 71.20.Be, 62.20.Fe

## I. INTRODUCTION

Many physical properties of crystalline materials, in particular plastic deformation and fracture, are controlled by extended defects such as dislocations and grain boundaries.[1] The strength of a grain boundary or the intrinsic mobility of dislocations, for example, are determined by their structures at the atomic scale. Over the last forty years, atomistic simulation has proven to be most adept in elucidating the structures and characteristics of extended defects in materials, along with their role in physical and mechanical properties.[2] Computer simulation naturally provides supreme control over the "experimental" conditions and also permits the often complex structures of defects to be visualized straightforwardly. Hence, it is free from many of the intrinsic limitations encountered by microscopy techniques. However, the fundamental question that must be asked of all atomistic simulations is the accuracy and transferability of the description of interatomic bonding used, i.e., how well does the model describe a given material and how trustworthy are its predictions when applied to crystal defects. In this paper, we will present an accurate and transferable model for interatomic bonding in the $5d$ transition metal iridium and we will demonstrate its suitability for use in the atomistic simulation of crystal defects in this material.

The mechanical properties of iridium are in many ways exceptional for a metal with the fcc crystal structure. Most notably, it is found that in tension single crystals fail by brittle transgranular cleavage at temperatures up to 500 °C after significant plastic deformation. In polycrystals, both transgranular cleavage and intergranular fracture are failure mechanisms, again after significant plastic deformation. Iridium is the only fcc metal to do so. This unusual behavior is most likely to be linked to the structure of dislocation cores[3] and/or grain boundaries in this material. For atomic level studies of such extended defects a reliable description of atomic interactions that can be employed in calculations encompassing several thousands of atoms is a prerequisite.

The development of interatomic potentials for iridium, and the transition metals in general, is challenging since it is essential to properly account for the angularly dependent bonding that arises from the valence $d$ electrons. Calculations based on density functional theory (DFT) are able to describe the electronic structure of any configuration of atoms very accurately but these methods still have severe limitations in studies of extended defects because only relatively small numbers of independent atoms $N$ can be included and that computational time scales as $O(N^3)$. For bulk materials, DFT methods require the machinery of Bloch's theorem to construct the electronic wave functions that leads to the requirement of periodic boundary conditions, which often is not convenient for studies of structures that exhibit low symmetry. It should be pointed out that in recent years DFT simulations of isolated dislocations in Mo (Ref. 4) and TiAl (Ref. 5) have been performed very successfully but these calculations required considerable computational resources and similar calculations could not be considered, for example, for detailed studies of dislocation motion or for defects with longer periods.

Empirical, many-body schemes in which an embedding function is constructed such that the bond energy of a given atom $E_{\text{bond}}^i$ is some function of the local atomic environment have been very successfully developed for a number of metallic systems. The most well-known schemes are the embedded atom method[6] (EAM) and Finnis-Sinclair potentials.[7] These potentials have been very widely used since they provide a relatively simple description of the many-body nature of cohesion in metals. However, these schemes assume central force bonding and thus are unable to describe the strong

angular dependencies of bonding in transition metals or transition metal-based intermetallics that arise from the partially filled $d$ band. Nevertheless, Finnis-Sinclair and EAM potentials have been developed for a number of transition metals, including iridium,[8,9] but they should be treated with caution since the effects of directional bonding are folded into the central force scheme in a way that cannot be adequately physically justified.

Iridium has unusual elastic constants in that its Cauchy pressure $C_{12}-C_{44}$ is small and negative.[10] In fact, iridium and the isoelectronic element rhodium are the only cubic elemental metals to exhibit negative Cauchy pressures.[11,12] As a result of the small magnitude of the Cauchy pressure in iridium, its elastic moduli can be quite well reproduced within a pairwise description of interatomic bonding since these interactions imply $C_{12}=C_{44}$ in the cubic case. Ivanov *et al.*[13] pursued this approach in the development of a model for interatomic bonding in iridium. However, as we will show later, cohesion in iridium exhibits very strong angular and many-body effects. Thus, while pairwise interactions imply zero Cauchy pressure, it is misleading to assume that the small magnitude of the Cauchy pressure suggests that a pairwise description of interatomic bonding is a good approximation.

Models for interatomic bonding based on the tight-binding (TB) approximation[14–18] to the full DFT expression for total energy constitute a scheme through which the many-body and angular dependencies of bonding in transition metals can be accurately described. Depending on the approximations made in the development of the TB scheme, such methods can be computationally efficient while maintaining the predictive power associated with a rigorous quantum-mechanical derivation. In this paper we will employ one such TB scheme, namely, the bond-order potential (BOP) formalism[19–21] which is a real-space, $O(N)$, orthogonal TB scheme. It was advanced by Pettifor and co-workers who have shown it to be eminently suitable for the atomistic simulation of extended defects in transition metals,[22–24] transition metal-based intermetallics,[25] and covalently bonded materials.[26] In the following section we summarize briefly the BOP scheme and in the subsequent section describe in detail the construction of the BOP for iridium. The remainder of the paper is then devoted to the testing of this BOP with the aim to demonstrate that it is transferable to environments significantly different from the ideal fcc lattice and thus suitable for atomistic modeling of extended crystal defects. We demonstrate the latter point by the calculation of the core structure of the screw dislocation in iridium, the results of which led to the development of a model for the unusual mechanical properties of iridium.[3]

## II. BOND-ORDER POTENTIALS

In the BOP formalism, the total energy $E_{tot}$ is written as a sum of three terms[24,25,27]

$$E_{tot} = E_{bond} + E_{env} + E_{pair}, \tag{1}$$

where $E_{bond}$ describes the cohesion that originates from the formation of a valence band when the atoms are brought together, $E_{env}$ is a many-body repulsive term that is used to fit Cauchy pressures,[28] and $E_{pair}$ is a pairwise interaction that includes all interactions not explicitly covered in the bond or many-body repulsive terms but mainly serves to provide short-range repulsion.[15] The many-body repulsive and pairwise terms will be discussed in detail in subsequent sections.

Using the standard result,[16–18] the bond energy is written as

$$E_{bond} = \sum_{i,j \neq i} \sum_{\alpha,\beta} \Theta_{j\beta,i\alpha} H_{i\alpha,j\beta}, \tag{2}$$

where $i$ and $j$ label atoms, $\alpha$ and $\beta$ label orbitals, and $\Theta$ and $H$ are the bond-order and Hamiltonian matrices, respectively, in the basis of real, orthonormal free-atom-like states $|i\alpha\rangle$.[20] In the two-center approximation, the off-diagonal elements of the Hamiltonian matrix are the usual Slater-Koster bond integrals.[14,29] The diagonal elements of the Hamiltonian are adjusted self-consistently during a simulation to enforce the condition of local charge neutrality. Due to the very short screening lengths in metals, the requirement of local charge neutrality is physically intuitive and allows for a rapid computation of forces via the Hellmann-Feynman theorem.[30] The force acting on atom $k$ with position vector $\mathbf{R}_k$ arising from the bond term is then

$$\mathbf{F}_k^{bond} = - \sum_{i,j \neq i} \sum_{\alpha,\beta} \Theta_{j\beta,i\alpha} \nabla_{\mathbf{R}_k} H_{i\alpha,j\beta}. \tag{3}$$

In the evaluation of the bond-order, we dispense with direct matrix diagonalization or $k$-space integration as is common in TB calculations (for example, Sutton *et al.*[31]). Instead, we utilize the concept of the exact many-body expansion for the bond-order[19,21] and the Lanczos recursion algorithm.[32] A complete discussion of this method is provided in Horsfield *et al.*[20] A finite electron temperature $T_e$ is introduced via the Fermi-Dirac distribution to ensure the numerical stability of the method and to smooth long-range Friedel oscillations.[33] We find optimum results with $k_B T_e = 0.3$ eV.

## III. CONSTRUCTION OF A BOND-ORDER POTENTIAL FOR IRIDIUM

The BOP formalism is a semiempirical scheme, meaning that the three terms in Eq. (1) contain adjustable parameters that are fitted to experimental or *ab initio* data. All semiempirical schemes must then be carefully tested to ensure they are transferable to structures that were not fitted explicitly. The BOP for iridium was parametrized sequentially starting with the bond term followed by the many-body repulsive term and finally the pairwise interaction. A small set of experimental and *ab initio* data was used in the fitting and at each stage of the parametrization we aimed to justify our methods and procedures physically. In this section we will provide a detailed description of the parametrization along with a critical discussion of the various approximations we have adopted.

### A. Construction and parametrization of bond term

The construction and parametrization of $E_{bond}$ requires that (i) the appropriate basis functions, i.e., $s$, $p$, $d$, or some

combination of these are selected (note that more basis functions lead to a more computationally demanding model); (ii) the radial dependencies of the bond integrals are established; (iii) the band filling, or number of electrons per atom, is determined, and (iv) the appropriate number of recursion levels $N_{rec}$ in the evaluation of the bond-order via the Lanczos recursion algorithm is ascertained. $N_{rec}$ should be chosen so that the BOP is able to reproduce the most important trends in structural stability, elastic constants, etc., when compared with $k$-space TB, bearing in mind that fewer recursion levels lead to greater computational efficiency. These four steps in the construction of the BOP are discussed in detail in the forthcoming sections.

### 1. Basis functions

The physical properties of the transition metals are dominated by the cohesion mediated by the valence $d$ electrons.[34] Well-known trends in structural stability and cohesive energy are observed as the $d$ band is filled with electrons[18] and moreover the $d$ electrons then impart a strong angular character to the interatomic bonding. The $sp$ electrons provide around 1 eV atom$^{-1}$ to the cohesive energy across the transition metal series but do not lead to strong angularly dependent bonding. It is therefore customary in the development of TB models for the transition metals to include only $d$ electrons explicitly in the bond term and describe the contribution of the nearly free (NFE) $sp$ electrons through a central force term (see, for example, Ref. 35).

We have studied the trends in structural stability as the $d$ band is filled with electrons using the *ab initio* linear muffin-tin orbital[36] (LMTO) method within the atomic sphere approximation including the combined correction. Structural energy differences were calculated using the frozen potential approximation[37–39] (FPA) whereby we first self-consistently calculated the ground-state charge density $\rho_{fcc}^{sc}$ and the corresponding atomic sphere potentials and densities of states (DOS) $n_{fcc}(E)$, for fcc iridium at the calculated equilibrium volume per atom. We then used the atomic sphere potentials ascertained self-consistently for the fcc structure in calculations of the total energy and DOS of the bcc and hcp lattices (throughout this paper, the hcp structure has the ideal $c/a$ ratio) at the same volume per atom but without self-consistently updating the potential (i.e., keeping the potential frozen). This frozen potential corresponds to a trial charge density $\rho^t$ and the error in the calculated energy compared with the value evaluated self-consistently is of second order in $\rho^t - \rho^{sc}$. Structural energy differences $\Delta$ may then be written as

$$\Delta = \int^{E_F} E n(E) dE - \int^{E_F} E n_{fcc}(E) dE, \qquad (4)$$

where $E_F$ is the Fermi energy and $n(E)$ represents the DOS calculated for the alternative crystal structures using a frozen potential.

The dependencies of the hcp-fcc and bcc-fcc structural energy differences on the number of electrons per atom $N$ calculated from the total $spd$ DOS for iridium, is presented in Fig. 1(a). This plot shows that at the band filling corresponding to iridium, $N=9$, the fcc structure is most stable. At this band filling, the hcp-fcc energy difference is relatively large, around 200 meV atom$^{-1}$, implying a large intrinsic stacking fault energy in this material that is confirmed by experiment[40] and *ab initio* calculations.[41,42] We also observe the close-packed-bcc-close-packed trend in structural stability as the band filling increases across the non-magnetic tran-
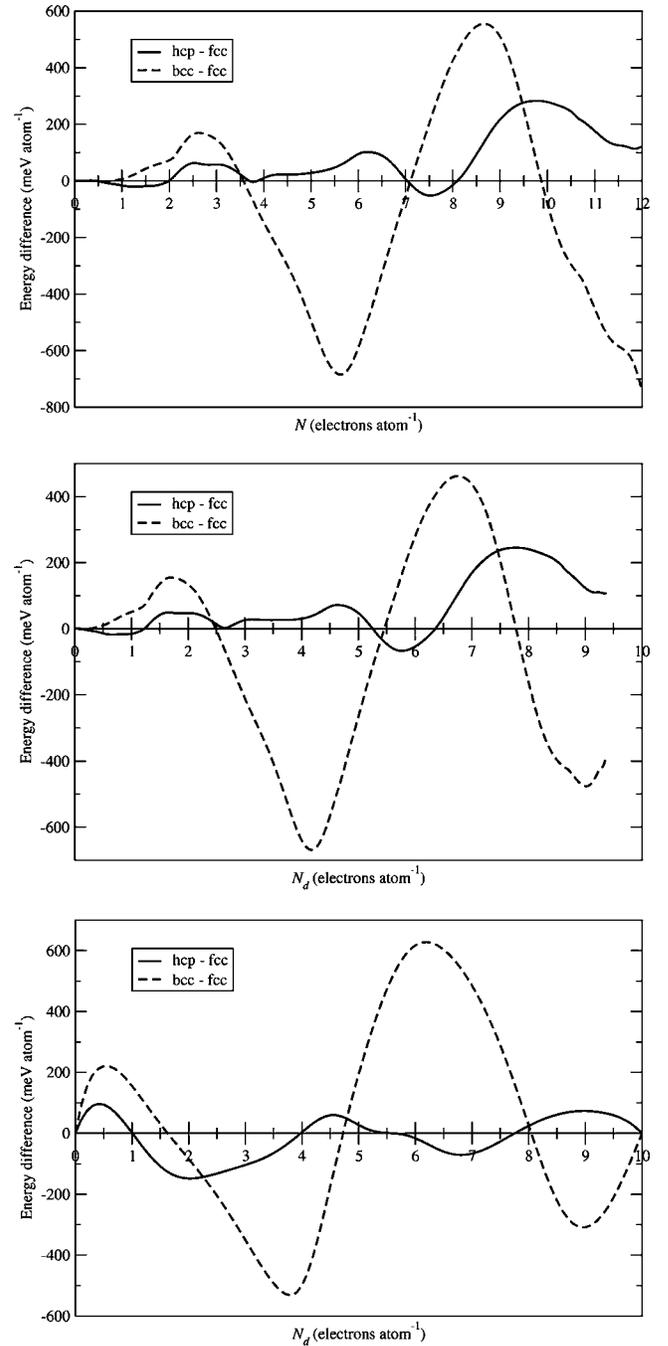


FIG. 1. Dependencies of hcp-fcc and bcc-fcc energy differences on band filling (a) as functions of total band filling calculated using LMTO and FPA from the total $spd$ DOS for iridium (b) as functions of $d$ band filling calculated using LMTO and FPA resolved into contribution from $d$ band (c) as a function of $d$ band filling calculated using $k$-space TB for a $d$ band with no hybridization with the $sp$ band.

sition elements, which is attributed to the large fourth moment contribution of the bcc structure.[16,18] The hcp-fcc and bcc-fcc structural energy differences calculated using Eq. (4) and the $d$ orbital partial DOS resolved from the $spd$ electron calculations are presented as a function of the $d$ band filling in Fig. 1(b). In this plot, a band filling of $N_d$=7.1 electrons per atom corresponds to iridium, as determined by our LMTO calculations. We ascribe the noninteger band filling to the effects of hybridization.The correspondence between Figs. 1(a) and 1(b) verifies that the valence $d$ electrons are responsible for the major trends in structural stability in the transition metals.

The LMTO calculations on which the structural energy difference presented in Figs. 1(a) and 1(b) are based include explicitly the effects of hybridization between the $s$, $p$, and $d$ orbitals. In contrast, calculations performed using a canonical $d$ band where hybridization between the $d$ electrons and the NFE $sp$ band is not included, as in Ref. 39, do not predict correctly the structural stability of the late transition elements. In Fig. 1(c), we plot the dependencies of the hcp-fcc and bcc-fcc structural energy differences on $N_d$ calculated using $k$-space integration of a TB Hamiltonian that includes only $d$ electrons. The volume per atom in each structure is now equal to the experimental volume per atom in the fcc structure, i.e., $3.839^3/4$ Å$^3$. The $dd\sigma$, $dd\pi$, and $dd\delta$ bond integrals, described in detail in the next section, were evaluated by applying the orbital downfolding technique to the results of self-consistent $spd$-orbital LMTO calculations for fcc iridium. This plot, along with the results presented in Refs. 39 and 21, indicates that a basis containing only $d$ electrons does predict correctly the fourth moment driven close-packed-bcc-close-packed trend in structural stability but it does not predict the correct stable close-packed structure, particularly for $N_d \geqslant 7$. The fcc structure is found to be most stable for $7.75 \leqslant N_d \leqslant 8$ but in this range, the energy differences between the fcc and both the bcc and hcp structures are not in good agreement with the results presented in Figs. 1(a) and 1(b). Furthermore, we found that band fillings in this range produced interatomic potentials that were a poor description of the properties of fcc iridium and displayed very limited transferability to other structures. In the development of the BOP, guided by our LMTO calculations, we used a $d$ band filling of $N_d$=7.1 electrons per atom. At this band filling, the bcc-fcc energy difference from an unhybridized $d$ band calculated using $k$-space TB is in excellent agreement with the results of the FPA calculations, although the hcp structure is predicted to be more stable than the fcc structure.

The role of $pd$ and $sd$ interactions in the determination of the hcp-fcc energy difference in iridium were studied by employing an $spd$ electron TB model [from Figs. 1(a) and 1(b), it is evident that $ss$ and $pp$ interactions do not affect this energy difference appreciably]. The $spd$ electron TB Hamiltonian was constructed by determining the radial dependencies of the bond integrals $ss\sigma$ through $dd\delta$ using the procedure described in the Sec. III A 2 while their angular dependencies were given by the usual Slater-Koster form.[14] The energies of the hcp and fcc structures were calculated at the experimental volume per atom by $k$-space integration of the TB Hamiltonian and the total energy difference was de-

composed into bond energy differences associated with each of the two-center integrals along with the corresponding promotion energies at a band filling of $N$=9. This decomposition of the hcp-fcc energy difference verified that it is only weakly dependent on the $ss\sigma$, $pp\sigma$, and $pp\pi$ interactions and, similarly, we also found that the $sd\sigma$, $pd\sigma$, and $pd\pi$ interactions do not provide any significant contribution. This decomposition suggested that the fcc structure is stabilized primarily by the $dd\pi$ and $dd\sigma$ interactions at first nearest neighbors and that the contribution from the bonds of $dd\delta$ character are negligible. The contributions of the first nearest neighbor $dd\pi$ and $dd\sigma$ bonds to the energy difference between the hcp and fcc structures were 81.8 and 29.7 meV atom$^{-1}$, respectively.

In order to investigate the applicability of the $d$ bond model employed in the development of the BOP, we also decomposed the hcp-fcc energy difference into the corresponding $dd\sigma$, $dd\pi$, and $dd\delta$ bond energies differences at first and second nearest neighbors via $k$-space integration of a TB Hamiltonian constructed from only $d$ electrons at a band filling of $N_d$=7.1. The radial dependencies of the $dd\tau$ ($\tau = \sigma, \pi, \delta$) bond integrals were the same as those used in the $spd$ electron Hamiltonian and thus any differences in the $dd\tau$ bond energies when compared with the $spd$ electron calculations were due to changes in the corresponding bond-order matrix elements because of the inclusion of additional basis functions of $s$ and $p$ character and the effects of hybridization. At the band filling corresponding to iridium, the hcp structure was favored by both the $dd\pi$ and $dd\sigma$ interactions, where the first nearest neighbor hcp-fcc bond energy differences are $-12.1$ and $-31.9$ meV atom$^{-1}$, respectively. In concurrence with the results of the $spd$ electron model, (i) the energy difference is overwhelmingly determined by the $dd\sigma$ and $dd\pi$ bonds formed at first nearest neighbors, (ii) the $dd\pi$ bonds at first nearest neighbors favor the fcc structure more strongly than the corresponding $dd\sigma$ bonds, and (iii) the contribution of the $dd\delta$ bonds to the energy difference was found to be negligible. Hence, the relative values of the $dd\tau$ bond energy differences provide strong evidence that the $d$ electron only model does accurately describe the angular characteristics of interatomic bonding at first nearest neighbors, in comparison with the $spd$ electron model, although the hcp-fcc energy difference is of the incorrect sign.

We found that the effects of hybridization between the $d$ band and the NFE $sp$ band can be approximated to an excellent extent by the addition of a pairwise, central force term in the total energy. By terminating the pairwise term beyond third nearest neighbors in the fcc lattice, we found it could be parametrized such that it makes up the difference between the hcp-fcc energy difference calculated from the bond term and the value determined *ab initio*. Since the $sp$ band gives rise to no strong angular dependencies and given that we have demonstrated conclusively that the hcp-fcc energy difference arises entirely from $d$ electrons, albeit under the influence of hybridization with the NFE band, the use of a central force term to approximate the effects of this hybridization in a $d$ electron only model is quite reasonable. In this manner, the total energies of the fcc and hcp structures are affected, but not the angular dependencies of interatomic bonding at short range. In the development of the BOP for

iridium, we have incorporated this pairwise interaction with the pairwise term described in Sec. III C.

Using a basis of only $d$ electrons in calculating the bond energy and emulating the effects of $sp$-$d$ hybridization with a pairwise, central force term, we have also ensured that the model is computationally efficient. The explicit inclusion of $s$ and $p$ basis functions in the TB Hamiltonian would result in a more computationally demanding scheme. This becomes particularly pronounced when the BOP formalism is adopted since the width of the NFE $sp$-band around a factor of 2 greater than that of the $d$ band and thus the number of levels in the Lanczos recursion chain would have to be doubled.

### 2. Radial dependencies of bond integrals

The radial dependencies of bond integrals $h_{ll'\tau}(R)$ were determined by employing the first-principles TB-LMTO method which utilizes a small basis of atom-centered, short-ranged orbitals. This was done by applying the orbital downfolding technique to a self-consistent TB-LMTO electronic structure calculation for iridium and evaluating the integrals numerically for different volumes of the fcc unit cell. For implementation into the BOP scheme, the dependence of the bond integrals on the radial distance between the atoms needs to be represented analytically by a continuous and differentiable function. For this purpose we have adopted the Goodwin-Skinner-Pettifor (GSP) function[43] $S_{ll'\tau}(R)$, such that

$$h_{ll'\tau}(R) = h_{ll'\tau}(R_0)S_{ll'\tau}(R) \tag{5}$$

and

$$S(R) = \left(\frac{R_0}{R}\right)^n \exp\left\{n\left[\left(\frac{R_0}{R_c}\right)^{n_c} - \left(\frac{R}{R_c}\right)^{n_c}\right]\right\}, \tag{6}$$

where we have suppressed the subscripts $ll'\tau$ in Eq. (6) for clarity. Here $R_0$ is the first nearest neighbor spacing in the ideal lattice and $R_c$, $n$, and $n_c$ are adjustable parameters. The angular dependencies of the bond integrals are given by the usual Slater-Koster form.[14] The GSP functions are augmented by a polynomial of fifth order beyond a certain distance $R_1$ in order to achieve a smooth cutoff at $R_{cut}$. The introduction of a cut-off tail is important to ensure the interactions remain short ranged.

Since the bond part is constructed from a basis of only $d$ electrons, there are only three bond integrals to be fitted, $dd\sigma$, $dd\pi$, and $dd\delta$. These bond integrals are cut-off at $R_{cut} = 4.3$ Å which is between second and third nearest neighbors in the fcc lattice and the cut-off tail is added at $R_1 = 3.3$ Å. The parametrization of the three GSP functions is given in Table I. In Fig. 2 we plot the radial dependencies of bond integrals described by Eq. (5), along with their values evaluated using first-principles TB-LMTO.

### 3. Number of recursion levels

The number of exact recursion levels employed in the Lanczos continuous fraction when evaluating the bond-order $N_{rec}$ affect significantly the accuracy and computational cost of the model, thus it is essential that the proper compromise

TABLE I. Parametrization of the GSP functions for iridium $dd\tau$ bond integrals.

| $ll'\tau$ | $h_{ll'\tau}(R_0)$ (eV) | $R_0$ (Å) | $n$ | $R_c$ (Å) | $n_c$ |
|---|---|---|---|---|---|
| $dd\sigma$ | −1.35966 | 2.714583 | 1.75339 | 3.30 | 3.71958 |
| $dd\pi$ | 0.564208 | 2.714583 | 1.70200 | 3.30 | 5.32968 |
| $dd\delta$ | −0.0646463 | 2.714583 | 1.83500 | 3.30 | 7.97587 |

is reached. From the point of view of forming chemical bonds between neighbors, atoms that are very distant exert little influence and thus very long hopping paths provide little additional information regarding the shape of the DOS. Therefore, the use of relatively a small number of levels in the Lanczos recursion chain can, particularly in the case of a small band width, provide excellent convergence to the full $k$-space results while also providing a computationally efficient, real-space model.

In Fig. 3 we plot the hcp-fcc and bcc-fcc energy differences as functions of the filling of the $d$ band calculated using $k$-space integration of the TB Hamiltonian [as in Fig. 1(c)] and BOP formalism at four levels of Lanczos recursion, at which all hopping paths of length nine are explicitly included. It is evident that an excellent agreement with the full $k$-space result is achieved in this case. Nastar and Willaime[44] demonstrated that the major trends in the elastic properties of the transition metals are reproduced when only five moments of the DOS were included in their $d$ electron TB model. Thus the use of four recursion levels in the BOP for iridium assures both excellent accuracy and computational efficiency.

### B. Parametrization of many-body repulsive term

Only $E_{bond}$ and $E_{env}$ have nonzero contributions to Cauchy pressures in the BOP formalism since they involve many-body interactions while $E_{pair}$ does not contribute.[29] Previous studies have shown that the many-body cohesion arising
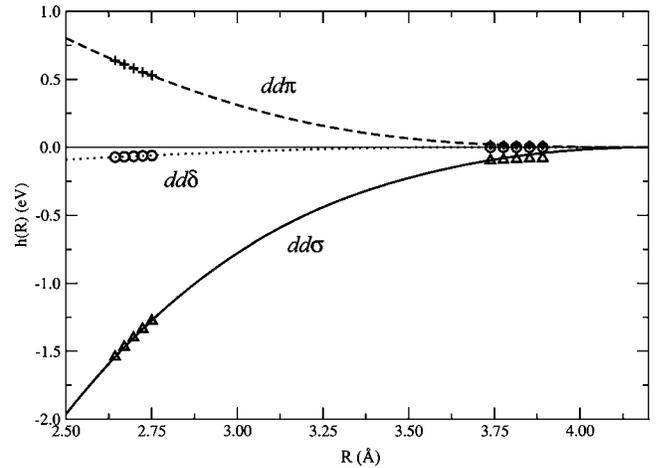


FIG. 2. The radial dependencies of the $dd\sigma$, $dd\pi$, and $dd\delta$ bond integrals in fcc iridium. The symbols correspond to the results of first-principles TB-LMTO calculations. The lines are the best fits made using the Goodwin-Skinner-Pettifor function [Eq. (6)].
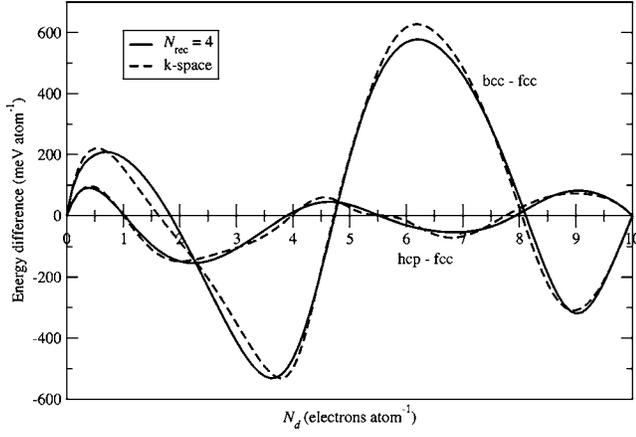
FIG. 3. hcp-fcc and bcc-fcc energy differences calculated as a function of $d$ band filling using $k$-space TB and the BOP formalism at four levels of Lanzcos recursion.

from $E_{bond}$ produces Cauchy pressures that are generally in poor agreement with the results of *ab initio* calculation or experiment and, moreover, are always positive. For many years it was believed that deficiencies in the description of cohesion led to these poor predictions for the elastic properties. However, systematic FP-LMTO calculations have shown that this is not the case.[28] Instead, it was found that the negative Cauchy pressures exhibited by metals such as iridium and rhodium and many transition metal-based intermetallic compounds arise from a many-body repulsive term. This term represents physically the overlap repulsion experienced by the $sp$ electrons when they are squeezed into the ion-core regions by the strong cohesion provided by the $d$ electrons.[45]

It was proposed by Nguyen-Manh *et al.*[28] to represent the many-body repulsive term within the BOP formalism as a screened Yukawa potential (see also Refs. 24 and 25)

$$E_{env} = \frac{1}{2} \sum_{i,j \neq i} B \frac{\exp[-\lambda(R_{ij} - 2R_{core})]}{R_{ij}}, \quad (7)$$

where

$$\lambda = \lambda_0 + \left[ \sum_{k \neq i} C \exp(-\nu R_{ik}) \right]^{1/\gamma} \quad (8)$$

and $B$, $\lambda_0$, $\nu$, $C$, and $\gamma$ are fitting parameters. $R_{core}$ is related to the radius of the valence $s$ orbital. As in the case of the radial dependencies of the bond integrals, the many-body repulsive term is augmented by a polynomial cut-off tail to ensure it decreases to zero smoothly.

The many-body repulsive term is parametrized to make up the difference between the Cauchy pressure given by the bond part and its experimental value. The Cauchy pressure given by the bond term is 0.3776 eV Å$^{-3}$ and the parametrization given in Table II enabled us to fit the experimental value of the Cauchy pressure exactly. The cut-off tail was added at 3.1 Å and was terminated at 4.2 Å.

TABLE II. Parametrization of the many-body repulsive term.

| $B$ (eV) | $\lambda_0$ (Å$^{-1}$) | $\nu$ (Å$^{-1}$) | $C$ (Å$^{-\gamma}$) | $\gamma$ | $R_{core}$ (Å) |
|---|---|---|---|---|---|
| 37.21 | 2.0 | 1.5 | 110.0 | 2.0 | 1.0 |

### C. Parametrization of pairwise interaction

The final term to be parametrized in our sequential fitting procedure is the pairwise interaction $E_{pair}$. This term represents all of the contributions to interatomic bonding that are not explicitly included in the preceding two terms, although it mainly serves to provide short range repulsion.[15,29] The pairwise term takes the same form as in Ref. 24, namely, a sum of cubic splines

$$E_{pair} = \frac{1}{2} \sum_{i,j \neq i} \sum_{k=1}^{4} A_k (R_k - R_{ij})^3 H(R_k - R_{ij}), \quad (9)$$

where the index $k$ labels node points $R_k$, and coefficients $A_k$ that are fitting parameters and $H(x)$ the Heaviside step function. With this functional form, we ensure that the first and second derivatives are continuous everywhere and that the function smoothly decreases to zero at the cutoff distance.

The pairwise term is used to fit remaining elastic constants, the fcc lattice parameter and cohesive energy. Furthermore, we have selected the positions of the node points so that we are able to fit the hcp-fcc structural energy difference calculated *ab initio*. In this way the pairwise term is also used to make up the difference between the structural energy difference calculated using the bond and many-body repulsive terms and the first-principles calculated value. In this manner the pairwise central force interaction also represents the effects of the NFE-$d$ hybridization on the energy differences between different close-packed structures, as discussed in Sec. III A 1.

The parametrization of the pairwise term is presented in Table III. The corresponding pair potential is plotted in Fig. 4 which illustrates that it provides weak cohesion at second nearest neighbors and beyond. This can be physically justified by considering that it also represents the cohesive contributions from the NFE $sp$ band. The equilibrium properties of iridium fitted during the parametrization are summarized in Table IV. Each of these values were fitted exactly.

### IV. TESTING THE BOND-ORDER POTENTIAL

The reason for the development of the BOP is its use in studies of crystal defects such as dislocations, high-angle

TABLE III. Parametrization of the pairwise term.

| $k$ | $R_k$ (Å) | $A_k$ (eV Å$^{-3}$) |
|---|---|---|
| 1 | 3.36945 | 1.621484180452 |
| 2 | 4.40000 | −0.034464172823 |
| 3 | 5.23000 | 1.479986236465 |
| 4 | 5.33000 | −1.300753052492 |
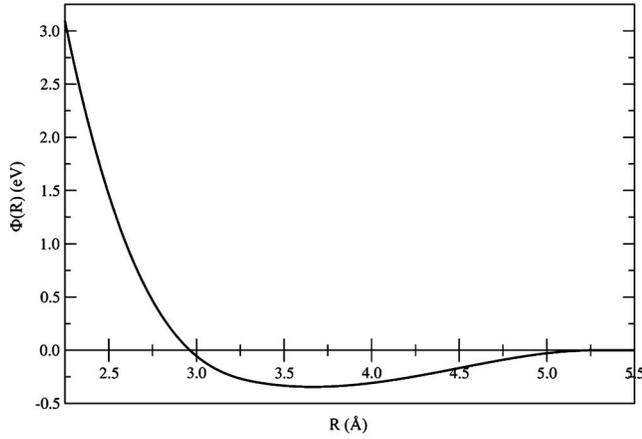
FIG. 4. Radial dependence of the pairwise term.



FIG. 5. Energy differences calculated as functions of volume per atom. The circles are the results of *ab initio* calculation where the atomic volumes have been normalized by the experimental volume per atom. The solid lines refer to the results of calculations made using the BOP.
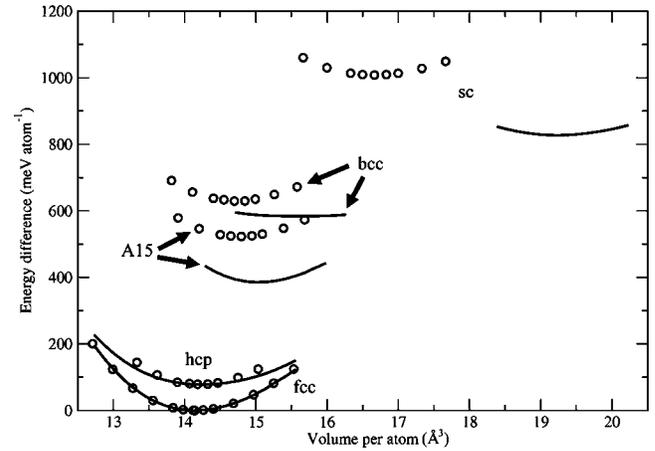
grain boundaries, vacancies, etc. Such defects generally result in a different local coordination than in the fcc lattice. Hence, the ability of the BOP to deal with structures with symmetries and coordination numbers that differ from those associated with the close-packed environment is important when assessing the situations to which the application of the BOP is appropriate. In order to test the transferability of the developed BOP, we performed the following calculations: (i) energy differences between the fcc and other crystal structures as functions of atomic volume, (ii) the tetragonal and trigonal deformation paths, and (iii) the phonon spectra of fcc iridium along three high symmetry directions. The results of the former two calculations are compared with identical calculations performed *ab initio* and the latter with experimental results. We also calculate the energies of some simple crystalline defects and compare these results with experiment and/or values calculated *ab initio*.

### A. Relative structural stability

The fcc-hcp energy difference was fitted during the construction of the potential but the transferability of the BOP to the more open $A15$, bcc, and simple cubic (sc) structures is of interest. The *ab initio* calculations of the energies of fcc, hcp, $A15$, bcc, and sc iridium were made using the mixed-basis, full potential augmented plane-wave plus local orbitals (APW+lo) method[48,49] as implemented in the WIEN2k package of codes.[50] The APW+lo calculations were all performed using the GGA xc functional of Perdew, Wang, and Ernzerhof[51] and the basis set was found to be optimized with

$R_{MT}K_{max}=10.5$ and $l_{max}=12$. An extra basis function of $d$ character was added at 2.25 Ry in order to increase the flexibility of the basis set. The muffin tin radius was set to 2.2 Bohr radii. The calculations used a $k$-point mesh of $36\times36\times36$ in the full Brillouin zone and were converged to a tolerance better than $10^{-6}$ Ry. Interestingly, our *ab initio* calculations found bcc iridium to be ferromagnetic in accordance with the Stoner theory of itinerant electron ferromagnetism.[52] At its equilibrium volume, our spin-polarized APW+lo calculations predict bcc iridium to have a magnetic moment of $0.553\mu_B$ atom$^{-1}$ corresponding to a reduction of energy compared with non-spin-polarized calculations of 20 meV atom$^{-1}$.

In Fig. 5 we present the dependencies of the energy difference relative to equilibrium fcc on atomic volume for the five structures under consideration calculated using the BOP and *ab initio*. We have normalized the atomic volumes predicted from *ab initio* calculations by the factor $(3.839/3.8276)^3/4$ in order to allow a direct comparison with the BOP results since in the BOP the volume per atom is fitted to the experimental value. As expected, the agreement between BOP and *ab initio* methods for the close-packed structures is excellent given that these were used in the parametrization. The transferability of the BOP to the open $A15$ and bcc structures is also good. It is seen that the energy differences and equilibrium volumes calculated using the

TABLE IV. Physical properties fitted during parametrization. Experimental and *ab initio* calculated values are reproduced exactly.

| $a$ (Å) | $E_{coh}$ (eV) | $C_{11}$ (eV Å$^{-3}$) | $C_{12}$ (eV Å$^{-3}$) | $C_{44}$ (eV Å$^{-3}$) | $E(hcp)-E(fcc)$ (meV atom$^{-1}$) |
|---|---|---|---|---|---|
| 3.839[a] | 6.93[b] | 3.620[c] | 1.510[c] | 1.598[c] | 78.8[d] |

[a]Reference 46.
[b]Reference 47.
[c]Reference 10.
[d]See Sec. IV A.

BOP and *ab initio* are the same within 5%. The transferability of the BOP to the sc structure is less satisfactory with an error of around 12% in the equilibrium atomic volume. However, the relatively poor transferability of the BOP to the sc structure is not of great concern since the energy of this structure is so high that it is extremely unlikely that it would ever occur in extended defects. The key result of this test is that the BOP predicts the same order of structural stability as *ab initio* calculations, i.e., fcc→hcp→A15→bcc→sc.

The transferability of the BOP for iridium to open crystal structures such as bcc could be significantly improved by the introduction of screening functions for the bond integrals.[24,53–55] Owing to the relatively small difference in separation of first and second nearest neighbors in such structures, the bond integrals are strongly environmentally dependent which in turn leads to significant discontinuities in their gradients between neighboring shells of atoms. The analytic screening functions advanced by Nguyen-Manh *et al.*[53] allow these environmental dependencies to be included into TB models and they were found to be critical in the development of BOPs for bcc metals such as molybdenum.[24] However, we have opted not to implement them for Ir since they do result in a notable increase in computational demand that cannot be justified in the study of defects in close-packed structures where the formation of such structures is highly unlikely.

It is possible that the errors in the predictions of the energy difference and equilibrium volume for the sc structure originate from the short-range repulsion provided by the pairwise and many-body repulsive terms in the BOP since the first nearest neighbor distance in the sc structure is very small (89% of the first nearest neighbor distance in the fcc structure at the same volume per atom). The short-range behavior of the potential is not fitted to any experimental or *ab initio* calculated property. Girshick *et al.*[22,23] attempted to ameliorate this weakness in the BOP formalism by ensuring that their BOP constructed for titanium fitted the "Rose curve" universal equation of state.[56,57] However, the success of such an approach cannot be judged since no comparison of energy differences between close-packed and open structured calculated using the constructed BOP and *ab initio* methods was reported in Refs. 22 and 23. The argument based on short interatomic distances in the sc structure is not entirely satisfactory because at the same atomic volume, the pairs of atoms on the cube faces in the A15 structure have the identical separation as first nearest neighbors in the sc structure. In the case of the BOP for iridium, the predictions of the A15-fcc energy difference and the equilibrium atomic volume of the A15 structure are in excellent agreement with *ab initio* calculations. It is interesting to point out that in molybdenum, when the BOP does not incorporate screening of the bond integrals,[24] the sc-bcc and A15-bcc energy differences are overestimated by factors of 1.5 and 3, respectively, when compared with *ab initio* calculations. This result does suggest that the short range behavior of the BOP is responsible for the observed errors. However, once the environmental dependencies of the bond integrals are incorporated into the BOP via the introduction of analytic screening functions, the sc-bcc energy difference predicted is in exact agreement with *ab initio* calculations while the error in the

prediction of the A15-bcc energy difference increases by a factor of 2. It appears difficult to attribute the poor prediction of the sc-fcc energy difference by the BOP for iridium to the short-range properties of the potential alone since the results in Ref. 24 indicate that the environmental dependencies of the bond part may also have a significant role to play.

## B. Tetragonal and trigonal deformation paths

A reliable test of the transferability of a scheme describing interatomic bonding to structures with reduced symmetry is the calculation of the energetics of deformation paths that can be directly compared with *ab initio* calculations.[24,58] Deformation paths are generated by applying a homogeneous strain that transforms one highly symmetric structure to another through intermediate structures that exhibit greatly reduced symmetry. In the present study, the tetragonal and trigonal deformation paths, described in detail in Ref. 58 have been studied.

The tetragonal deformation path, also known as the Bain path, transforms in an elemental solid the bcc lattice continuously to the fcc lattice. In this process the bcc lattice is strained parallel to [001] at constant volume and the parameter $p$, which is equal to the $c/a$ ratio of the corresponding intermediary tetragonal cell, is used to characterize the position along the deformation path. This corresponds to the homogeneous straining described by the Lagrange strain tensor of finite deformations

$$\varepsilon_{11} = \varepsilon_{22} = (p^{-2/3} - 1)/2,$$

$$\varepsilon_{33} = (p^{4/3} - 1)/2,$$

$$\varepsilon_{12} = \varepsilon_{13} = \varepsilon_{23} = 0 \qquad (10)$$

in the coordinate system where the $x$, $y$, and $z$ axes are parallel to the [100], [010], and [001] directions, respectively. The special points on the deformation path are $p=1$, which corresponds to the original bcc lattice, and $p=\sqrt{2}$, which corresponds to the fcc lattice. For the tetragonal deformation path, the difference in energy from the ground state structure vs $p$, calculated using the BOP and the *ab initio* full potential linear augmented plane-wave (FLAPW) method[59] is presented in Fig. 6.

The trigonal deformation path also continuously transforms the bcc lattice to the fcc lattice but passes through the sc structure. This path is described by the same Lagrange strain tensor as the tetragonal path but with the $x$, $y$, and $z$ axes parallel to [1$\bar{1}$0], [11$\bar{2}$], and [111], respectively. In this case, the cell is extended parallel to [111] at constant volume. Special points along the trigonal path are $p=1$, which corresponds to the bcc lattice $p=2$, which corresponds to the sc lattice and $p=4$ which corresponds to the fcc lattice. For the trigonal path, the results analogous to those shown in Fig. 6 are presented in Fig. 7.

Figures 6 and 7 show for both the tetragonal and trigonal deformation paths an outstanding agreement between calculations employing the BOP and the *ab initio* method. The transferability of the BOP to the bcc structure is very good
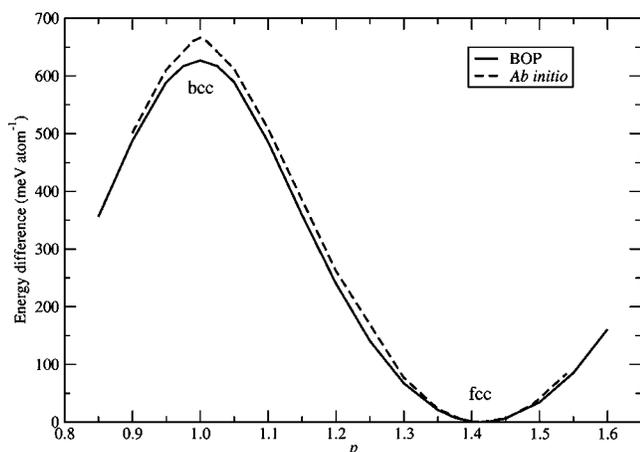
FIG. 6. The tetragonal deformation path calculated using BOP and first-principles methods. The structures at the special points on the path are indicated.

but larger errors are seen in the transferability to the sc structure, as also seen previously in Fig. 5. In the latter, the sc-fcc energy difference was determined at the equilibrium volume of the sc structure whereas in the calculation of the trigonal deformation path, the volume per atom of the sc structure is around 35% smaller than the equilibrium value. This is the reason for the significantly different values of the energies of the sc structure in Figs. 5 and 7, respectively. In contrast, the volume per atom of the bcc structure in Figs. 6 and 7 is only 4% smaller than the equilibrium value given by the minimum in the dependence of the energy of bcc iridium on atomic volume in Fig. 5. However, the purpose of the study of deformation paths is to compare the BOP and *ab initio* calculations for the same structures. The most notable outcome of this test is the overall close agreement between the predictions of the BOP and *ab initio* methods for the energy differences at intermediate points along both paths. Structures encountered at intermediate values of $p$ exhibit very little symmetry and thus provide an excellent assessment of the transferability of the BOP to crystal defects where the local symmetry and related bond angles and coordination
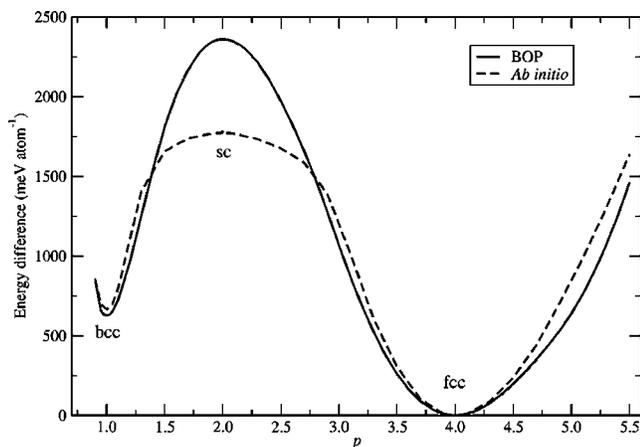


FIG. 7. The trigonal deformation path calculated using BOP and first-principles methods. The structures at the special points on the path are indicated.

numbers may differ significantly from the fcc environment.

In the calculation of the energetics of the trigonal path using the FLAPW method, the energy difference is observed to change relatively slowly as a function of the parameter $p$ in the range $1.4 \leqslant p \leqslant 3.0$. It is not possible to decompose the total energy calculated using first-principles methods such as FLAPW into purely cohesive and repulsive interactions, etc. Hence, we cannot offer a clear and unambiguous physical explanation for this behavior. The energy difference calculated using the BOP for iridium changes rapidly as function of $p$ in the same range which we attribute to the increasing contribution of the short range repulsion provided by the pairwise term as the interatomic distance decreases during the formation of the sc structure at $p=2$.

### C. Phonon spectra of iridium

The phonon spectra of a crystalline solid provide a wealth of information over all length scales—at long wavelengths the elastic properties of the lattice are examined while at short wavelengths the nature of interatomic bonding is directly probed. The calculation of phonon spectra is a particularly good test of an interatomic potential for these reasons. These calculations can also indicate any possible structural instabilities in the ground-state crystal structure by the presence of soft or imaginary branches.

The phonon spectra of iridium are particularly interesting since several anomalies are observed experimentally.[60] Specifically, in the $[\zeta\zeta0]$ branches, local minima and inflexion points are found that cannot be accounted for by crystal symmetry arguments and are likely to be due to the strong angular character of interatomic bonding in iridium.

We have calculated the phonon spectra of iridium along the $[\zeta00]$, $[\zeta\zeta0]$, and $[\zeta\zeta\zeta]$ directions using the method of frozen phonons.[61] These calculations were performed by making supercells of 20 periods of the underlying lattice along $[100]$, $[110]$, and $[111]$. The amplitude of the applied sinusoidal waves was 0.02 Å. Phonon frequencies were calculated at wave vectors corresponding to $\zeta=0.05n$ with $n=0,1,2,\ldots,20$ necessary to ensure the waves were commensurate with the supercell. At the wave vectors sampled, the mean square displacement was 0.0002 Å$^2$. The calculated phonon spectra along with experimental results from Heid *et al.*[60,62] are presented in Fig. 8.

The overall agreement between the calculations employing the BOP for iridium and experiment is excellent. Since the experimental elastic constants of iridium were fitted exactly, both sets of spectra are practically identical at long wavelengths. However, the agreement between experiment and theory at shorter wavelengths is also very good and thus provides a clear indication that the constructed BOP is a very good description of interatomic bonding in iridium.

A notable success of the BOP for iridium is its accurate prediction of the anomaly in the $[\zeta\zeta0]$ $T2$ branch starting around $\zeta=0.5$. In order to test that the inflexion is not due to an unphysical bump in any of the three terms in Eq. (1), we decomposed the phonon energy of this branch into its components from the bond, many-body repulsive and pairwise terms (Fig. 9). This decomposition demonstrates that the
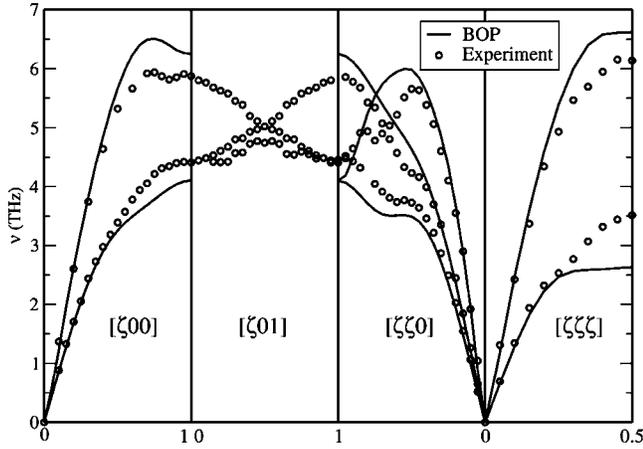
FIG. 8. The phonon spectra of iridium calculated using BOP by the method of frozen phonons along three high symmetry directions compared with experimental results (circles).

contribution to the phonon energy from the bond term increases more rapidly than the opposing contributions from the pairwise and many-body repulsive terms. Hence, it is likely that the atomic displacements associated with this phonon mode couple to the angular character of interatomic bonding in iridium in a particularly strong manner, leading to the observed anomalies.

The two degenerate transverse $[\zeta\zeta\zeta]$ branches are observed to soften at around $\zeta=0.25$. These phonon modes correspond to a shearing of {111} planes in the fcc lattice parallel to each other and so it is likely that this softening is related to the bond part in the BOP favoring the hcp structure over fcc. In spite of these relatively soft phonon branches, the calculated phonon spectra never suggest that the fcc lattice is unstable for some distortion of the lattice as none of the branches are observed to approach zero frequency.

### D. Stacking faults and vacancies

#### 1. Stacking faults

Using the constructed BOP, we have calculated the energies of the intrinsic and extrinsic stacking faults, along with
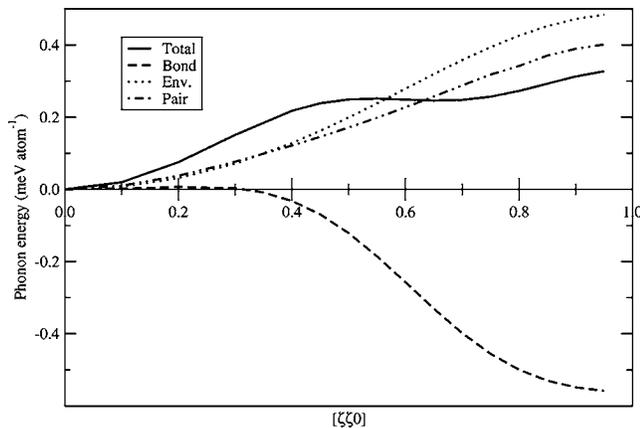


FIG. 9. The energy of the $[\zeta\zeta0]$ T2 phonon branch decomposed into the contributions from the bond, many-body repulsive, and pairwise terms.

the energy of the twin boundary. Blocks containing 156 atoms were used that were generated by stacking {111} planes in the appropriate order to form the stacking fault. Periodic boundary conditions were applied in the directions parallel to the plane of the stacking fault and/or twin boundary. Perpendicular to the plane of the fault, the block was divided into an active region of width $18\sqrt{3}a$ centered on the plane of the fault where atomistic relaxation was performed. The active region was sandwiched by regions of thickness $4\sqrt{3}a$ where the atoms were held fixed. This geometry of simulation cell ensures that the energy of an isolated stacking fault and/or twin boundary is calculated.

The agreement between the intrinsic stacking fault energy calculated using the BOP, 408 mJ m$^{-2}$, and experiment, 420 mJ m$^{-2}$ (Ref. 40), as well as with the range of values calculated *ab initio*, 365 (Ref. 41)–445 (this work) mJ m$^{-2}$, is very good. However, such good agreement is expected since the hcp-fcc structural energy difference is fitted during the parametrization of the BOP. It is important that the intrinsic stacking fault energy that the BOP produces is in such good agreement with experiment because of the role it plays in determining the equilibrium width of splitting of a dislocation into Shockley partials.[1]

We find the energies of the extrinsic stacking fault and twin boundary to be 462 and 222 mJ m$^{-2}$, respectively. There are no experimental or *ab initio* calculated values to compare with but the calculated energies do follow the expected trends based on the numbers of {111} layers that are not in perfect fcc registry, i.e., the energy of the twin boundary is around one half of that of intrinsic stacking fault and the energy of the extrinsic stacking fault is slightly higher than that of the intrinsic stacking fault.[1]

#### 2. Vacancy formation energy

The vacancy formation energy was calculated using supercells containing the vacancy at their center. The supercells were relaxed atomistically until the force acting on any atom was less than 0.01 eV Å$^{-1}$. The vacancy formation energy was then calculated according to the relation $E_{\mathrm{vac}}=E_{\mathrm{tot}}(N-1)-[(N-1)/N]E_{\mathrm{tot}}(N)$[63] where $N$ is the total number of atoms in the perfect supercell. In order to assure the independence of the calculated vacancy formation energy on block size, we gradually increased the size of the supercell until the vacancy formation energy was found not to vary further. This occurred for $N=864$ and we found the relaxed vacancy formation energy $E_{\mathrm{vac}}^{r}=2.97$ eV and the unrelaxed vacancy formation energy $E_{\mathrm{vac}}^{u}=3.42$ eV. The ratio $E_{\mathrm{vac}}^{u}/|E_{\mathrm{coh}}|=0.49$ is in excellent agreement with the simple arguments, presented in Ref. 18 regarding the numbers of broken and strengthened bonds that result from the formation of the vacancy. On the other hand, $E_{\mathrm{vac}}^{r}/|E_{\mathrm{coh}}|=0.43$ is not in good agreement with the results of *ab initio* calculations that report $E_{\mathrm{vac}}^{r}/|E_{\mathrm{coh}}|=0.27$ and 0.33 (Refs. 63 and 41, respectively). The origin of the discrepancies between the relaxed vacancy formation energy predicted by the BOP and those predicted by first-principles calculations is not clear. It is possible that owing to the relatively small numbers of atoms that can be included in DFT calculations, the atomic relaxations differ significantly from those in the larger cells used

in the BOP calculations, although higher energies would be expected from DFT calculations since less relaxation is possible. Hence, it is more likely that the BOP is unable to account for local changes in electronic structure around the vacancy that are properly captured in DFT calculations.[64] The inclusion of analytic screening functions for the bond integrals may improve the predictions for the vacancy formation energy in iridium,[24] assuming that the observed discrepancies are electronic in origin.

## V. APPLICATION OF BOP TO DISLOCATION CORE STRUCTURES

We applied the constructed BOP to the atomistic simulation of the core structure of the screw dislocation in iridium. The simulation block consisted of a cylinder one Burgers vector in height and of radius 60 Å. The axis of the cylinder is parallel to the dislocation line, i.e., $[1\bar{1}0]$, and periodic boundary conditions were applied in this direction. The block was divided into three regions: a central region of radius 30 Å (region I) containing the elastic center of dislocation within cylinders of thickness 12 Å (region II) and 18 Å (region III). The dislocation was introduced into to the center of the block by displacing all atoms in accordance with the corresponding strain field evaluated using anisotropic elasticity. The positions of atoms in region I were relaxed atomistically using the BOP until the force acting on any atom was less than 0.01 eV Å$^{-1}$. Atoms in the outer region of the block (regions II and III) were held fixed at their initial positions during the atomistic relaxation of region I. The incompatibility forces generated in region II during the atomistic relaxation of atoms in region I were used to update the positions of all atoms using the Green's function boundary condition (GFBC) formalism.[4,5,65–67] The use of the GFBC formalism allowed us to update self-consistently the boundary regions of the simulation block during atomistic relaxation of the dislocation core via iterations of atomistic relaxation of region I followed by a GFBC update.

We found two possible configurations for the core of the $a/2[1\bar{1}0]$ screw dislocation in iridium; a planar core that is spread only on the (111) plane, corresponding to dissociation into Shockley partials, and a nonplanar core that is spread onto the intersecting (111) and $(11\bar{1})$ planes of the $[1\bar{1}0]$ zone. In Fig. 10(a), the planar core structure is presented as a differential displacement map. The splitting between partials is extremely narrow at around 12 Å. This value is consistent with the HRTEM observations of Balk and Hemker.[40] The nonplanar configuration of the core of the screw dislocation is presented in Fig. 10(b). A comparison of the energies of the dislocations with these two different cores[3] showed that the dislocation with the nonplanar core is metastable and is higher in energy than the dislocation with the planar core by 0.33 eV $b^{-1}$. Such a metastable nonplanar core configuration has never previously been reported in atomistic simulations of fcc metals and it is likely to be unique to iridium because of the strong angular character of its interatomic bonding which is captured accurately by the constructed BOP.

It has been shown in a recent paper (Ref. 3) that the existence of a metastable nonplanar configuration for the
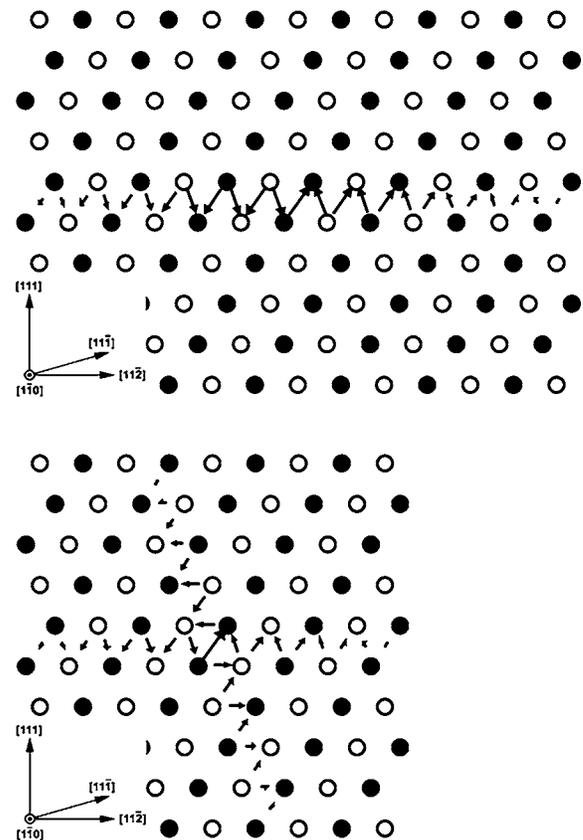


FIG. 10. Differential displacement maps of screw dislocation cores in iridium. In these figures, the circles depict atoms in the projection onto the plane perpendicular to the dislocation line $(1\bar{1}0)$ and the open and closed circles distinguish two planes of atoms within one period. The arrows represent relative displacement parallel to the total Burgers vector between two neighboring atoms. The length of the arrows is proportional to the magnitude of the displacement normalized by $a/2\sqrt{2}$, where $a$ is the fcc lattice parameter. (a) Planar core spread onto the (111) plane. (b) Nonplanar core spread onto the intersecting (111) and $(11\bar{1})$ planes.

screw dislocation core may have a significant effect on the mechanical properties of iridium. Stress driven transformations between the planar and nonplanar core configurations may occur and the nonplanar core configuration serves as an intermediate configuration for cross slip which then takes place without thermal activation. Such athermal cross slip, together with the high mobility of the dislocation with the planar core, gives rise to an anomalously high density of Frank-Read sources generated via the double cross slip mechanism[68] and leads subsequently to a dislocation density that increases exponentially with plastic strain. When the dislocation density in the material reaches the level at which the mean free path of dislocations is comparable to the magnitude of their Burgers vector, further dislocation glide is extremely difficult, stress concentrators cannot be relaxed via dislocation mediated plasticity and the material becomes brittle. These mechanisms, which can be related directly to the angular character of bonds in iridium, explain its unusual mechanical behavior.

## VI. DISCUSSION AND CONCLUSIONS

Several semiempirical models for the description of interatomic bonding in iridium have been developed. These range from pair potentials, through the embedded atom method to TB schemes. All of these methods do have their own strengths and weaknesses, however, in this paper we have demonstrated that the BOP we have developed is particularly suitable for use in the atomistic simulation of extended defects in iridium.

The EAM potential constructed by Chen[8] provides a reasonably good description of the equilibrium properties of fcc iridium but this is achieved through the use of an unphysical embedding function with negative curvature. This form of embedding function cannot be justified on the basis of electronic theory of metals. Neither pair potentials nor the EAM formalism describe the angular bonding that we have shown to be so important in the case of fcc iridium. While the EAM potential does provide accurate predictions for the vacancy formation energy and the lattice parameter of hypothetical bcc iridium, the bcc-fcc energy difference is only one third of the value found by our *ab initio* calculations. The latter is likely to be related to the neglect of angular bonding in the potential.

A modified-embedded atom method (MEAM) potential has been developed for iridium by van Beurden and Kramer.[69] This is an improvement over the pair potential and EAM schemes since it includes the effects of angular bonding in the embedding functions, albeit in an entirely empirical manner. While the MEAM formalism is significantly more computationally efficient than the BOP, this is at the expense of a significantly less rigorous relation to the fully quantum-mechanical description of interatomic bonding provided by TB methods. The embedding functions used in the MEAM, require fitting to more experimental or *ab initio* data than is the case with BOP. Thus, while the MEAM does provide a framework for the atomistic simulation of defects, it is likely that its transferability is significantly less comprehensive than that of the BOP.

Mehl and Papaconstantopoulos[70] have developed a TB description of interatomic bonding in iridium which uses an *spd* basis. As discussed in Sec. III A, such a scheme is likely to be both accurate and transferable to at least the same extent as the BOP. However, it is not a real-space method and so cannot be applied as straightforwardly as the BOP to structures exhibiting reduced symmetry. Furthermore, this TB scheme requires significantly more fitting parameters.

The BOP presented in this paper compares very favorably with other widely used and well-established methods, ranging from first-principles electronic structure calculations in terms of accuracy and transferability to empirical potentials in terms of their computational efficiency. First, it is fully quantum mechanically based, real space, and has relatively few adjustable parameters. It describes accurately the equilibrium properties of fcc iridium, such as its elastic constants, owing to the proper treatment of angular bonding and the introduction of a many-body repulsive term in the expression for the total energy. This potential also exhibits excellent transferability to structures that differ significantly from the fcc environment in both symmetry and coordination. This has been demonstrated through the calculation of energy differences between different structures as functions of atomic volume along with the energetics of the tetragonal and trigonal deformation paths. Most notably, the BOP yields excellent predictions for the phonon spectra, including certain anomalous features of the $[\zeta\zeta 0]$ branches. While the constructed BOP is computationally intensive and not well suited for very large-scale molecular dynamics or Monte Carlo simulations, it is proficient for the atomistic simulation of the structure and properties of crystalline defects, such as straight dislocations and periodic grain boundaries that require not more than a few thousands of atoms in the relaxed region. Indeed, we have demonstrated the efficacy of the BOP in atomistic studies of the screw dislocation in iridium. The planar core configuration for the screw dislocation was in excellent agreement with experimental results[40] and we predicted that a metastable, nonplanar core configuration. The results of these atomistic simulations allowed us to elucidate a mechanism for athermal cross slip that is unique to iridium and develop a model which accounts for the unusual mechanical properties of this material.[3]

*Present address: Explosives and Organic Materials (T-14), MS B221, Theoretical Division, Los Alamos National Laboratory, Los Alamos, New Mexico 87545, USA. Electronic address: cawkwell@lanl.gov

†Electronic address: duc.nguyen@ukaea.org.uk

‡Electronic address: vitek@lrsm.upenn.edu

[1] J. P. Hirth and J. Lothe, *Theory of Dislocations* (Wiley-Interscience, New York, 1982).

[2] *Handbook of Materials Modeling*, edited by S. Yip (Springer, Berlin, 2005).

[3] M. J. Cawkwell, D. Nguyen-Manh, C. Woodward, D. G. Pettifor, and V. Vitek, Science **309**, 1059 (2005).

[4] C. Woodward and S. I. Rao, Phys. Rev. Lett. **88**, 216402 (2002).

[5] C. Woodward and S. I. Rao, Philos. Mag. **84**, 401 (2004).

[6] M. S. Daw and M. I. Baskes, Phys. Rev. B **29**, 6443 (1984).

[7] M. W. Finnis and J. E. Sinclair, Philos. Mag. A **50**, 45 (1984).

[8] S. P. Chen, Philos. Mag. A **66**, 1 (1992).

[9] R. A. Johnson (private communication).

[10] R. E. MacFarlane, J. A. Rayne, and C. T. Jones, Phys. Lett. **20**, 234 (1966).

[11] O. Y. Kontsevoi, Y. N. Gornostyrev, and A. J. Freeman, JOM **57**, 43 (2005).

[12] D. Maurer, R. Heichele, N. Lingg, V. Muller, and K. H. Rieder, Phys. Status Solidi A **160**, 403 (1997).

[13] A. S. Ivanov, M. I. Katsnelson, A. G. Mikhin, Y. N. Osetskii, A. Y. Rumyantsev, A. V. Trefilov, Y. F. Shammanaev, and L. I. Yakovenkova, Philos. Mag. B **69**, 1183 (1994).

[14] J. C. Slater and G. F. Koster, Phys. Rev. **94**, 1498 (1954).

[15] A. P. Sutton, M. W. Finnis, D. G. Pettifor, and Y. Ohta, J. Phys. C **21**, 35 (1988).

[16] A. P. Sutton, *Electronic Structure of Materials* (Oxford University Press, Oxford, 1993).

[17] A. P. Sutton and R. W. Balluffi, *Interfaces in Crystalline Materials* (Oxford University Press, Oxford, 1995).

[18] D. G. Pettifor, *Bonding and Structure of Molecules and Solids* (Oxford University Press, Oxford, 1995).

[19] D. G. Pettifor, Phys. Rev. Lett. **63**, 2480 (1989).

[20] A. P. Horsfield, A. M. Bratkovsky, M. Fearn, D. G. Pettifor, and M. Aoki, Phys. Rev. B **53**, 12694 (1996).

[21] M. Aoki, Phys. Rev. Lett. **71**, 3842 (1993).

[22] A. Girshick, A. M. Bratkovsky, D. G. Pettifor, and V. Vitek, Philos. Mag. A **77**, 981 (1998).

[23] A. Girshick, D. G. Pettifor, and V. Vitek, Philos. Mag. A **77**, 999 (1998).

[24] M. Mrovec, D. Nguyen-Manh, D. G. Pettifor, and V. Vitek, Phys. Rev. B **69**, 094115 (2004).

[25] S. Znam, D. Nguyen-Manh, D. G. Pettifor, and V. Vitek, Philos. Mag. **83**, 415 (2003).

[26] A. P. Horsfield, P. D. Godwin, D. G. Pettifor, and A. P. Sutton, Phys. Rev. B **54**, 15773 (1996).

[27] D. Nguyen-Manh, D. G. Pettifor, D. J. H. Cockayne, M. Mrovec, S. Znam, and V. Vitek, Bull. Mater. Sci. **26**, 43 (2003).

[28] D. Nguyen-Manh, D. G. Pettifor, S. Znam, and V. Vitek, in *Tight-Binding Approach to Computational Materials Science*, edited by P. E. A. Turchi, A. Gonis, and L. Colombo (Materials Research Society, Warrendale, Boston, MA, 1998), Vol. 491, p. 353.

[29] M. W. Finnis, *Interatomic Forces in Condensed Matter* (Oxford University Press, Oxford, 2003).

[30] R. P. Feynman, Phys. Rev. **56**, 340 (1939).

[31] A. P. Sutton, T. N. Todorov, M. J. Cawkwell, and J. Hoekstra, Philos. Mag. A **81**, 1833 (2001).

[32] C. Lanczos, J. Res. Natl. Bur. Stand. **45**, 255 (1950).

[33] A. P. Horsfield and A. M. Bratkovsky, Phys. Rev. B **53**, 15381 (1996).

[34] J. Friedel, in *The Physics of Metals*, edited by J. M. Ziman (Cambridge University Press, New York, 1969), p. 494.

[35] A. T. Paxton, J. Phys. D **29**, 1689 (1996).

[36] O. K. Andersen, Phys. Rev. B **12**, 3060 (1975).

[37] D. G. Pettifor, Commun. Phys. (London) **1**, 141 (1976).

[38] D. G. Pettifor, J. Chem. Phys. **69**, 2930 (1978).

[39] H. L. Skriver, Phys. Rev. B **31**, 1909 (1985).

[40] T. J. Balk and K. J. Hemker, Philos. Mag. A **81**, 1507 (2001).

[41] Y. N. Gornostyrev, M. I. Katsnelson, N. I. Medvedeva, O. N. Mryasov, A. J. Freeman, and A. V. Trefilov, Phys. Rev. B **62**, 7802 (2000).

[42] N. M. Rosengaard and H. L. Skriver, Phys. Rev. B **47**, 12865 (1993).

[43] L. Goodwin, A. J. Skinner, and D. G. Pettifor, Europhys. Lett. **9**, 701 (1989).

[44] M. Nastar and F. Willaime, Phys. Rev. B **51**, 6896 (1995).

[45] D. G. Pettifor, J. Phys. F: Met. Phys. **8**, 219 (1978).

[46] L. B. Hunt, Platinum Met. Rev. **31**, 32 (1987).

[47] C. Kittel, *Introduction to Solid State Physics* (Wiley, New York, 1996).

[48] E. Sjöstedt, L. Nordström, and D. J. Singh, Solid State Commun. **114**, 15 (2000).

[49] G. K. H. Madsen, P. Blaha, K. Schwarz, E. Sjöstedt, and L. Nordström, Phys. Rev. B **64**, 195134 (2001).

[50] P. Blaha, K. Schwarz, G. K. H. Madsen, D. Kvasnicka, and J. Luitz, *WIEN2k, An Augmented Plane Wave + Local Orbitals Program for Calculating Crystal Properties* (Karlheinz Schwarz, Technische Universität Wien, Austria, 2001).

[51] J. P. Perdew, K. Burke, and M. Ernzerhof, Phys. Rev. Lett. **77**, 3865 (1996).

[52] J. Kübler, *Theory of Itinerant Electron Magnetism* (Oxford University Press, New York, 2000).

[53] D. Nguyen-Manh, D. G. Pettifor, and V. Vitek, Phys. Rev. Lett. **85**, 4136 (2000).

[54] M. Mrovec, Ph.D. Thesis, University of Pennsylvania, 2002.

[55] H. Haas, C. Z. Wang, M. Fähnle, C. Elsässer, and K. M. Ho, Phys. Rev. B **57**, 1461 (1998).

[56] J. H. Rose, J. R. Smith, and J. Ferrante, Phys. Rev. B **28**, 1835 (1983).

[57] J. H. Rose, J. R. Smith, F. Guinea, and J. Ferrante, Phys. Rev. B **29**, 2963 (1984).

[58] V. Paidar, L. G. Wang, M. Sob, and V. Vitek, Modell. Simul. Mater. Sci. Eng. **7**, 369 (1999).

[59] M. Sob, L. G. Wang, and V. Vitek, Comput. Mater. Sci. **8**, 100 (1997).

[60] R. Heid, K. P. Bohnen, K. Felix, K. M. Ho, and W. Reichardt, J. Phys.: Condens. Matter **10**, 7967 (1998).

[61] P. K. Lam and M. L. Cohen, Phys. Rev. B **25**, 6139 (1982).

[62] R. Heid (private communication).

[63] P. A. Korzhavyi, I. A. Abrikosov, B. Johansson, A. V. Ruban, and H. L. Skriver, Phys. Rev. B **59**, 11693 (1999).

[64] G. Jacucci, R. Taylor, A. Tenenbaum, and N. van Doan, J. Phys. F: Met. Phys. **11**, 793 (1981).

[65] J. E. Sinclair, P. C. Gehlen, R. G. Hoagland, and J. P. Hirth, J. Appl. Phys. **49**, 3890 (1978).

[66] S. Rao, C. Hernandez, J. P. Simmons, T. A. Parthasarathy, and C. Woodward, Philos. Mag. A **77**, 231 (1998).

[67] C. Woodward and S. I. Rao, Philos. Mag. A **81**, 1305 (2001).

[68] J. S. Koehler, Phys. Rev. **86**, 52 (1952).

[69] P. van Beurden and G. J. Kramer, Phys. Rev. B **63**, 165106 (2001).

[70] M. J. Mehl and D. A. Papaconstantopoulos, Phys. Rev. B **54**, 4519 (1996).